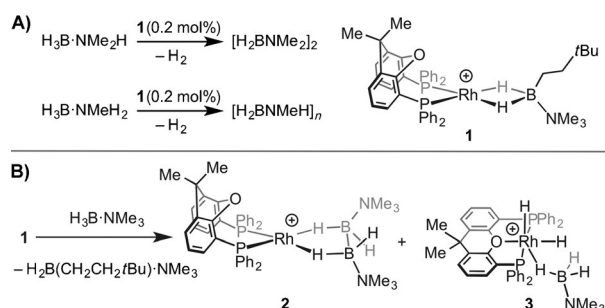


P–C-Activated Bimetallic Rhodium Xantphos Complexes: Formation and Catalytic Dehydrocoupling of Amine–Boranes**

Heather C. Johnson* and Andrew S. Weller*

Abstract: $\{Rh(xantphos)\}$ -based phosphido dimers form by P–C activation of xantphos (4,5-bis(diphenylphosphino)-9,9-dimethylxanthene) in the presence of amine–boranes. These dimers are active dehydrocoupling catalysts, forming polymeric $[H_2BNMeH]_n$ from $H_3B\cdot NMe_2H$ and dimeric $[H_2BNMe_2]_2$ from $H_3B\cdot NMe_2H$ at low catalyst loadings (0.1 mol%). Mechanistic investigations support a dimeric active species, suggesting that bimetallic catalysis may be possible in amine–borane dehydrocoupling.

The catalytic dehydrocoupling of amine–boranes^[1] has received much attention with regard to hydrogen storage applications (e.g. $H_3B\cdot NH_3$)^[2] or as a means to form BN-based materials, such as polyaminoboranes $[H_2BNRH]_n$ ($R = H, Me, nBu$), through catalytic dehydropolymerization.^[3] We have recently reported the complex $[Rh(\kappa^2\text{-PP-xantphos})\{\eta^2\text{-}H_2B(CH_2CH_2tBu)\cdot NMe_3\}][BAR^F_4]$ **1** ($Ar^F = 3,5\text{-}(CF_3)_2C_6H_3$, xantphos = 4,5-bis(diphenylphosphino)-9,9-dimethylxanthene), which acts as a source of the $\{Rh(xantphos)\}^+$ fragment.^[4] Complex **1** is an active catalyst for the dehydropolymerization of $H_3B\cdot NMe_2H$ to form $[H_2BNMeH]_n$ of moderate molecular weight ($M_n = 22700\text{ g mol}^{-1}$, PDI = 2.1; PDI = polydispersity index), as well as for the dehydrocoupling of $H_3B\cdot NMe_2H$ to form $[H_2BNMe_2]_2$ (Scheme 1 A).^[4] Kinetic data indicate an induction period involving rate limiting N–H activation and that saturation kinetics operate during productive catalysis, suggesting an active catalyst that has an amidoborane motif which binds a subsequent equivalent of amine–borane. However, the precise structure of this active species remains unclear. Complex **1** also promotes the stoichiometric B–B homocoupling of $H_3B\cdot NMe_3$ to form $[Rh(\kappa^2\text{-PP-xantphos})(H_4B_2\cdot 2NMe_3)][BAR^F_4]$ **2** alongside the dihydride complex $[Rh(\kappa^3\text{-P,O,P-xantphos})(H)_2(\eta^1\text{-}H_3B\cdot NMe_3)][BAR^F_4]$ **3** (Scheme 1 B)^[5] and also promotes the hydroboration of alkenes using $H_3B\cdot NMe_3$.^[6]



Scheme 1. A) Catalytic dehydrocoupling of $H_3B\cdot NMe_2H$ and $H_3B\cdot NMe_2H$ with **1**. B) Homocoupling of $H_3B\cdot NMe_3$ using **1**. $[BAR^F_4]^-$ ions are not shown.

We now report that at the end of amine–borane dehydrocoupling using catalyst **1**, Rh_2 dimeric complexes are isolated in which a xantphos ligand has undergone P–C activation.^[7] Surprisingly this dimeric motif also acts a very active precatalyst, suggesting the possibility for cooperative bimetallic reactivity^[8] in the dehydropolymerization of amine–boranes.^[9]

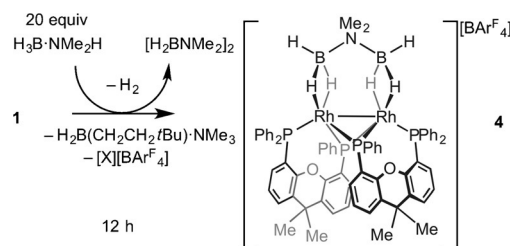
Addition of **1** (5 mol%) to $H_3B\cdot NMe_2H$ in a 1,2- $C_6H_4F_2$ solution (sealed NMR tube) resulted in the rapid formation of a Rh^{III} dihydride sigma amine–borane complex, an induction period before the onset of catalysis, and the observation (65% consumption, 3 h) of a resting state tentatively assigned to an amidoborane complex.^[4] Investigation of the reaction mixture at a late stage of the catalytic process (> 90% consumption, 4.5 h) revealed a new complex that became the major organometallic product after 12 h (Scheme 2). Isolation as an orange crystalline material in 40% yield (based on Rh), and analysis by single-crystal X-ray diffraction, NMR spectroscopy, and ESI-MS show this to be a xantphos-derived P–C-activated phosphido-bridged Rh_2 dimer with a coordinated N,N -dimethylaminodiboranate: $[Rh_2(\kappa^2\text{-PP-xantphos})_2(\eta^2, \eta^2\text{-}H_3BNMe_2BH_3)][BAR^F_4]$ **4** (Figure 1).

[*] Dr. H. C. Johnson, Prof. A. S. Weller
 Department of Chemistry, University of Oxford
 Mansfield Road, Oxford, OX1 3TA (UK)
 E-mail: andrew.weller@chem.ox.ac.uk

[**] We thank the EPSRC for funding and Dr. George Whittell (University of Bristol) for GPC analysis. Xantphos = 4,5-bis(diphenylphosphino)-9,9-dimethylxanthene.

Supporting information for this article is available on the WWW under <http://dx.doi.org/10.1002/anie.201504073>.

© 2015 The Authors. Published by Wiley-VCH Verlag GmbH & Co. KGaA. This is an open access article under the terms of the Creative Commons Attribution License, which permits use, distribution and reproduction in any medium, provided the original work is properly cited.



Scheme 2. The formation of complex **4** at 5 mol% catalyst loadings. The identity of $[X][BAR^F_4]$ was not determined.

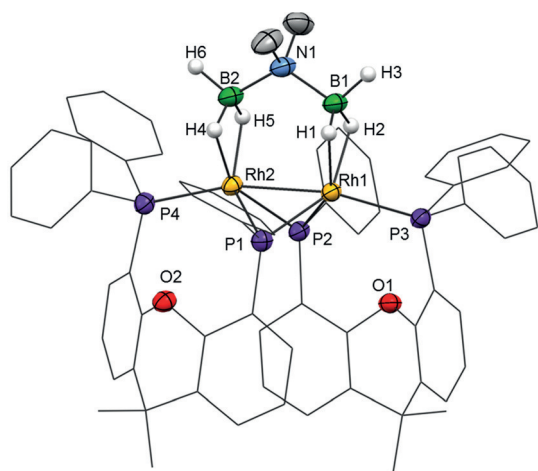
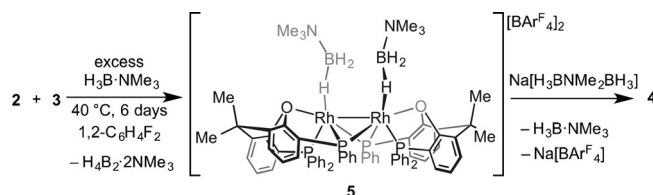


Figure 1. Solid-state structure of the cationic component of **4**. Displacement ellipsoids are set at 50% probability. H atoms bound to C centers are omitted for clarity, and the carbon atoms in the xantphos' ligands are depicted as a wireframe. Selected bond lengths [Å] and angles [°]: Rh1–Rh2 2.5928(4), Rh1–P1 2.2455(12), Rh1–P2 2.2500(11), Rh1–P3 2.3427(11), Rh2–P1 2.2461(11), Rh2–P2 2.2663(11), Rh2–P4 2.3325(11), Rh1–B1 2.234(5), Rh2–B2 2.229(5), Rh1–O1 3.393(4), Rh2–O2 3.412(4), B1–N1 1.600(7), N1–B2 1.583(7); P1–Rh2–P4 114.64(4), P2–Rh1–P3 110.89(4), B1–N1–B2 117.5(4).

These data reveal that the xantphos ligands have undergone a P–C activation, forming two bridging phosphido groups (4-phenylphosphido-5-diphenylphosphino-9,9-dimethylxanthene, xantphos') which span the Rh–Rh vector (Figure 1). Each xantphos' ligand is bound in a κ^2 -P,P configuration and the central Rh₂P₂ unit adopts a butterfly geometry.^[10] A [H₃BNMe₂BH₃][−] ion^[11,12] bridges the two metal centers. The B–H hydrogen atoms were located, and each BH₃ group is bound η^2 to the metal center (Rh–B 2.234(5), 2.229(5) Å). A Rh–Rh single bond is proposed,^[13] and although the distance of 2.5928(4) Å might thus be considered short,^[14] the Rh₂P₂ unit appears fairly flexible to the requirements of the bridging ligands as the Rh–Rh distances in complexes **5** and **7** (see below) are longer. The NMR spectroscopic data (CD₂Cl₂) are fully consistent with the solid-state structure. Two environments are detected in the ³¹P{¹H} NMR spectrum with resonance signals at δ = 108.5 (virtual tt) and δ = 13.3 ppm (virtual ddt) assigned to the phosphido and phosphino groups, respectively, on the basis of chemical shifts and coupling constants.^[15,16] The ¹¹B NMR spectrum shows a broad resonance at δ = 16.6 ppm corresponding to the BH₃ groups, shifted circa 29 ppm downfield compared to Na[H₃B·NMe₂·BH₃] (δ = −12.5 ppm, q, THF),^[11] suggesting a significant interaction with the metal.^[17] Signals attributable to the bridging Rh–H–B hydrides in **4** are detected at δ = −2.68 and δ = −3.52 ppm in the ¹H NMR spectrum, whereas signals for the terminal B–H groups are detected at δ = 4.14 ppm. These signals sharpen in the ¹H{¹¹B} NMR spectrum, and the observation of three different environments in a 1:1:1 ratio shows that the BH₃ unit is static on the NMR timescale. Complex **4** is best considered as a 26-electron {Rh(κ^2 -P,P-xantphos')}₂²⁺ fragment coordi-

nated with [H₃BNMe₂BH₃][−]. Bimetallic complexes with bridging amine- or phosphine–borane-derived ligands are rare.^[9b,18]

The P–C-activated {Rh(xantphos')}₂²⁺ motif observed in **4** can also be formed by heating a 1:1 mixture of complexes **2** and **3** (Scheme 1, generated in situ^[5]) at 40 °C for 6 days. This reaction results in the formation, in quantitative yield (determined by NMR spectroscopy), of [Rh₂(κ^3 -P,O,P-xantphos')₂(η^1 -H₃B·NMe₃)₂][BAr^F₄]₂ **5** (Scheme 3). Although similar to **4**, the solid-state structure (Figure 2) shows that each H₃B·NMe₃ binds in a η^1 configuration with the metal center and the xantphos' adopts a κ^3 -P,O,P bonding motif. There is a crystallographically imposed twofold axis of symmetry in the cation. The Rh–Rh distance of 2.7965(5) Å is significantly longer than in **4** (2.5928(4) Å), reflecting the difference in monodentate and bridging ligands respectively, whereas the Rh–B distance of 2.722(4) Å shows η^1 amine–borane binding. The solution NMR data for **5** are consistent with the solid-state structure.^[16] In the ³¹P{¹H} NMR spectrum two environments are detected, δ = 135.1 (virtual tt) and δ = 19.2 ppm (virtual ddt), whereas in the ¹H NMR spectrum signals for the H₃B groups are detected as a broad signal at δ = −0.39 ppm (relative integral 6H). This suggests rapid exchange between the bridging and terminal B–H groups, and cooling to 200 K did not result in splitting of this signal. The ¹¹B NMR



Scheme 3. Formation of complex **5** and subsequent reaction to form complex **4**.

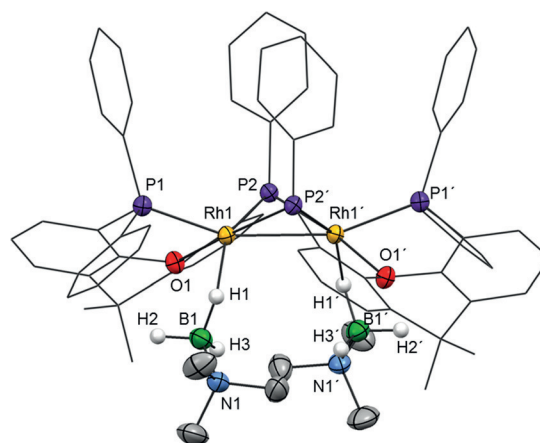
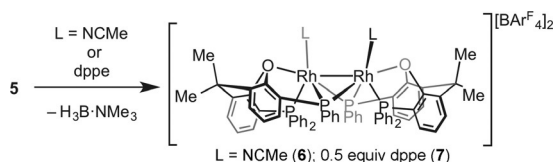


Figure 2. Solid-state structure of the cationic component of **5**. Displacement ellipsoids are set at 50% probability. H atoms bound to C centers are omitted, and the carbon atoms in the chelating ligand backbone are depicted as a wireframe. Selected bond lengths [Å] and angles [°]: Rh1–Rh1' 2.7965(5), Rh1–P2' 2.1940(9), Rh1–P2 2.2192(8), Rh1–P1 2.3344(9), Rh1–O1 2.288(2), Rh1–B1 2.722(4), N1–B1 1.594(5); P2–Rh1–P1 119.72(3), Rh1–P2–Rh1' 78.64(3), Rh1'–Rh1–P2' 51.08(2), Rh1'–Rh1–P2 50.28(2).

spectrum displays a broad signal at $\delta = -7.8$ ppm, barely shifted from that of free $\text{H}_3\text{B}\cdot\text{NMe}_3$. All these data are consistent with η^1 -coordination of the amine–borane being retained in solution.^[17,19] Complex **4** can also be formed by reaction of **5** with $\text{Na}[\text{H}_3\text{BNMe}_2\text{BH}_3]$, revealing that the xantphos' ligand can adopt a flexible coordination mode^[20] in response to the requirements of the amine–borane ligands.

The σ -bound $\text{H}_3\text{B}\cdot\text{NMe}_3$ ligands in **5** can also be easily displaced by addition of MeCN or $\text{Ph}_2\text{PCH}_2\text{CH}_2\text{PPh}_2$ (dppe) to form $[\text{Rh}_2(\kappa^3\text{-P,O,P-xantphos})_2(\text{L})_2][\text{BAR}^{\text{F}}_4]_2$ **6** ($\text{L} = \text{MeCN}$) or **7** ($\text{L}_2 = \text{dppe}$), respectively (Scheme 4). In both cases, the



Scheme 4. Formation of complexes **6** and **7**.

Rh_2 -based dimeric unit remains intact, as shown by NMR spectroscopy. The solid-state structure of **7** confirms the $\{\text{Rh}(\text{xantphos})\}_2$ motif, showing a $\kappa^3\text{-P,O,P}$ geometry and a bridging dppe ligand.^[16] The Rh–Rh distance in **7** is 2.8362(5) Å, longer than in both **4** and **5**. Addition of $\text{H}_3\text{B}\cdot\text{NMe}_2\text{H}$ (4 equiv) to **5** results in dehydrocoupling to form $[\text{H}_2\text{BNMe}_2]_2$ and a 1:1 mixture of **4:5**.

Although not fully resolved, there are clues to the mechanism of formation of these dimers. During the formation of **5**, no intermediates were detected by NMR spectroscopy, whereas benzene and biphenyl were detected in a circa 3:1 ratio by GC–MS in the final reaction mixture, consistent with P–aryl bond cleavage and subsequent elimination. The requirement for both Rh^{I} and Rh^{III} fragments is demonstrated by the fact that heating Rh^{I} -based complex **2** to 40 °C with excess $\text{H}_3\text{B}\cdot\text{NMe}_3$ for one week ($1,2\text{-C}_6\text{H}_4\text{F}_2$) did not produce **5**, but addition of **3** to excess $\text{H}_3\text{B}\cdot\text{NMe}_3$ formed **5** quantitatively (6 days, 40 °C), during which signals for the formation of small amounts of **2** were detected by NMR spectroscopy. Under an atmosphere of H_2 (4 atm), which would favor Rh^{III} dihydride species,^[4] the conversion is slower, roughly 30% in 6 days. Combination of $[\text{Rh}(\kappa^3\text{-P,O,P-xantphos})(\text{H})_2(\text{NCMe})][\text{BAR}^{\text{F}}_4]$ ^[21] and $[\text{Rh}(\kappa^3\text{-P,O,P-xantphos})(\text{PCy}_3)][\text{BAR}^{\text{F}}_4]$ ^[6] at 40 °C for 5 days resulted in essentially no change, which suggests that rather labile ligands and/or amine–borane are required for dimer formation. We speculate that low-coordinate Rh^{I} $\{\text{Rh}(\text{xantphos})\}^+$ and Rh^{III} $\{\text{Rh}(\text{xantphos})(\text{H})_2\}^+$ fragments formed in situ combine to form a complex with bridging hydrides, such as, for example, $[\text{Rh}_2(\text{xantphos})_2(\mu\text{-H})_2(\text{H}_3\text{B}\cdot\text{NMe}_3)_n][\text{BAR}^{\text{F}}_4]_2$. From this, P–C activation of xantphos occurs with subsequent elimination of benzene or biphenyl/ H_2 . Although there are many reports of the P–C activation of phosphines to form phosphido bridges,^[7,22] this is, to our knowledge, the first instance of such a process occurring with the xantphos ligand. P–C activation of xantphos has been reported from $[\text{Pd}(\kappa^3\text{-P,O,P-xantphos})(\text{closo-SnB}_{11}\text{H}_{11})]$ to form a direct P–B bond.^[23]

The formation of phosphido bridges during homogeneous catalysis is generally considered a catalyst deactivation route.^[7,25] However, examples of such species acting as precatalysts in a variety of transformations are known,^[26] and there is evidence suggesting that in this system dimers do play a role. The dehydrocoupling of $\text{H}_3\text{B}\cdot\text{NMe}_2\text{H}$ catalyzed by **5** was investigated using conditions which were the same as those described for monomer precatalyst **1** (0.2 mol%, open system).^[4] Addition of **5** (0.1 mol%; i.e. 0.2 mol% $[\text{Rh}]$) to $\text{H}_3\text{B}\cdot\text{NMe}_2\text{H}$ formed $[\text{H}_2\text{BNMe}_2]_2$ with $\text{H}_2\text{B}=\text{NMe}_2$ as the major boron-containing intermediate detected (Figure 3A). There is an induction period of circa 300 s prior to productive catalysis (turnover frequency (TOF) 2300 h^{-1} , 1150 h^{-1} relative to $[\text{Rh}]$; compared with circa 1000 h^{-1} using **1**). Turnover continued after addition of excess Hg to the reaction mixture, suggesting homogeneous catalysis. Upon varying the initial $[\text{H}_3\text{B}\cdot\text{NMe}_2\text{H}]$ across the range 0.288–0.018 M, system behavior broadly suggestive of saturation kinetics was measured (post-induction period): at $[\text{H}_3\text{B}\cdot\text{NMe}_2\text{H}]$ above circa 0.1 M,

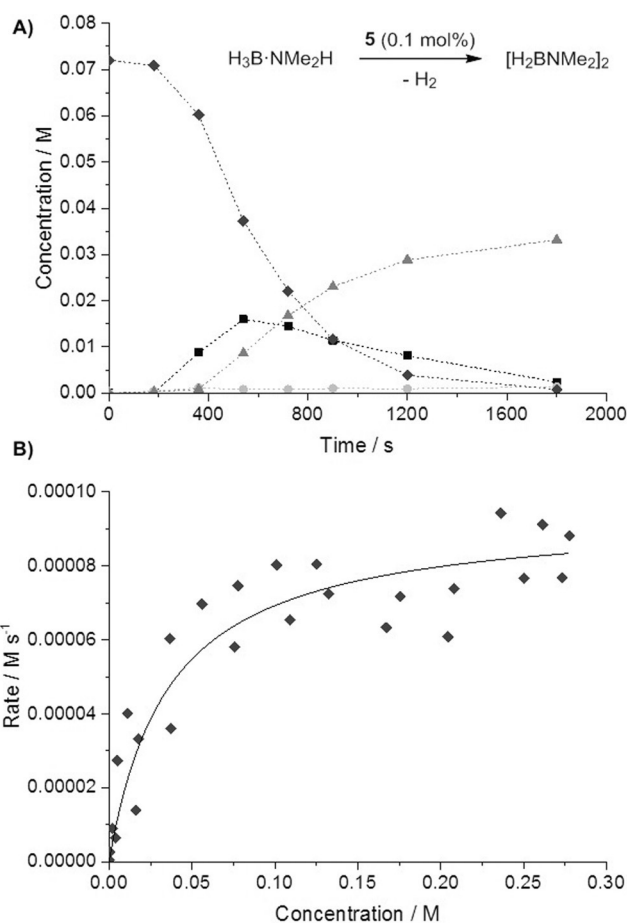
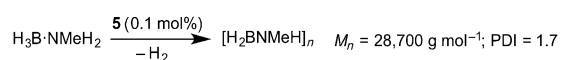


Figure 3. A) Concentration versus time plots (as measured by ^{11}B NMR spectroscopy) for species $\text{H}_3\text{B}\cdot\text{NMe}_2\text{H}$ (\blacklozenge , black), $\text{H}_2\text{B}=\text{NMe}_2$ (\blacksquare , black), $\text{HB}(\text{NMe}_2)_2$ (\bullet , light gray), and $[\text{H}_2\text{BNMe}_2]_2$ (\blacktriangle , dark gray). Conditions: $[\text{H}_3\text{B}\cdot\text{NMe}_2\text{H}]_0 = 0.072$ M, $[\mathbf{5}] = 7.2 \times 10^{-5}$ M, $1,2\text{-C}_6\text{H}_4\text{F}_2$ was used as solvent, open conditions, 298 K. B) Plot of rate versus $[\text{H}_3\text{B}\cdot\text{NMe}_2\text{H}]$ for the dehydrocoupling of $[\text{H}_3\text{B}\cdot\text{NMe}_2\text{H}]$ by **5**, showing the post-induction period. Separate experiments spanning the range 0.288–0.018 M were carried out. The line of best fit is to guide the eye only.^[24]

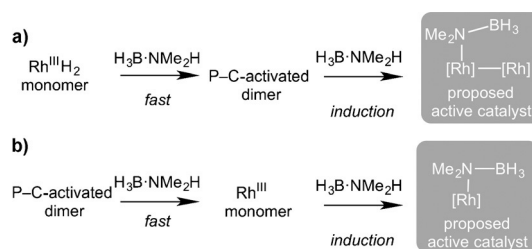
pseudo-zero-order decay of $[\text{H}_3\text{B}\cdot\text{NMe}_2\text{H}]$ was measured, while approximate pseudo-first-order consumption of $\text{H}_3\text{B}\cdot\text{NMe}_2\text{H}$ was found at lower concentrations (Figure 3 B). Similar saturation kinetics were previously shown with **1**.^[4] During the early stages of catalysis, post-induction, the measured rate shows a first order dependence on **5**, rather than half order that would suggest a rapid dimer–monomer equilibrium in which the dimer lies off-cycle.^[27]

Kinetic isotope effects of 1.1 ± 0.2 and 2.0 ± 0.3 were measured by using $\text{D}_3\text{B}\cdot\text{NMe}_2\text{H}$ and $\text{H}_3\text{B}\cdot\text{NMe}_2\text{D}$ respectively (zero-order regions), suggesting that N–H activation may be involved in, or in an equilibrium prior to, the turnover-limiting step. Moreover, the induction period approximately doubled from about 300 s with $\text{H}_3\text{B}\cdot\text{NMe}_2\text{H}$ and $\text{D}_3\text{B}\cdot\text{NMe}_2\text{H}$ to circa 600 s with $\text{H}_3\text{B}\cdot\text{NMe}_2\text{D}$, indicating that N–H activation is also involved in the rate-limiting process during the formation of the catalytically active species. Consistent with labelling experiments, B–H activation in **5** is fast and reversible as addition of D_2 to **5** results in incorporation of D into the BH_3 groups within the time of mixing, possibly via a $\sigma\text{-CAM}$ -type process ($\sigma\text{-CAM} = \sigma\text{-complex-assisted meta-thesis}$).^[28] These observations combined suggest that the active catalytic species contains an N–H-activated amine–borane, possibly an amidoborane complex, that quasi-reversibly coordinates a second equivalent of $\text{H}_3\text{B}\cdot\text{NMe}_2\text{H}$. The dehydrocoupling of $\text{H}_3\text{B}\cdot\text{NMe}_2\text{H}$ (0.072 M, $[\mathbf{5}] = 7.2 \times 10^{-5} \text{ M}$) in a sealed system, which enables build-up of H_2 , shows a TOF of circa 450 h^{-1} (relative to $[\text{Rh}]$), slower than in the open system, indicating inhibition by H_2 . The decay of $[\text{H}_3\text{B}\cdot\text{NMe}_2\text{H}]$ follows a first-order profile (post-induction period), again very similar to that seen with **1** under the same conditions.^[4] Complex **4** is also active in catalysis, but shows a longer induction period and a slower overall rate.^[16] Complex **5** (0.1 mol %) also catalyzes the dehydropolymerization of $\text{H}_3\text{B}\cdot\text{NMe}_2\text{H}$ to form $[\text{H}_2\text{BNMeH}]_n$ ($M_n = 28700 \text{ g mol}^{-1}$, PDI = 1.7, Scheme 5). This is a similar molecular weight to the $[\text{H}_2\text{BNMeH}]_n$ produced under analogous conditions with **1** ($M_n = 22700 \text{ g mol}^{-1}$, PDI = 2.1).^[4]



Scheme 5. Dehydropolymerization of $\text{H}_3\text{B}\cdot\text{NMe}_2\text{H}$ using **5** as a catalyst.

Overall, these studies suggest that the mechanism of the dehydrocoupling of amine–boranes by **5** and **1** at low catalyst loadings (0.2 mol % Rh) are likely closely related: both **1** and **5** show induction periods as well as very similar kinetic profiles and isotope effects. We postulate that the active species, whether a monomer or dimer, is accessed through N–H activation. Complex **4** that was isolated at the end of catalysis could form from the addition of BH_3 to a $[\text{Rh}]_2\text{NMe}_2\text{BH}_3$ unit. As shown in Scheme 6, we propose that the active species forms by one of two pathways: a) P–C activation in a Rh^{III} complex related to **3** (which would result from addition of $\text{H}_3\text{B}\cdot\text{NMe}_2\text{H}$ to **1**^[4]) that is very fast under conditions of a high relative amine–borane concentration and forms a dimeric species related to **5** that then



Scheme 6. Proposed pathways for the formation of the active catalyst under conditions of high relative $[\text{H}_3\text{B}\cdot\text{NMe}_2\text{H}]$ (500 equiv) starting from a) monomeric and b) dimeric precatalysts.

undergoes a slower N–H activation to form a dimeric active species; or b) the monomeric species are the active catalysts, which could be formed when starting from **5** by opening up of the phosphido bridges, perhaps by protonation by the amine–borane. To explore this latter possibility, complex **5** was reacted with HCl (Et_2O solution) and MeI. In both cases intractable mixtures resulted. Unfortunately ESI-MS, or crossover experiments using different xantphos-containing precursors, have not been definitive in discounting either the dimer or the monomer as the active species. Catalysis in a sealed NMR tube with 20 equivalents of $\text{H}_3\text{B}\cdot\text{NMe}_2\text{H}$ (5 mol % $[\text{Rh}]$) was employed to probe likely resting states. During catalysis, ^1H and $^{31}\text{P}\{^1\text{H}\}$ NMR spectra showed broad unresolved signals, suggestive of several species, while after 12 h, complex **4** was again the major organometallic product formed. Under these conditions of higher catalyst loading, dimer **5** is strikingly faster than monomer **1** (TOF 240 h^{-1} and 4 h^{-1} ,^[4] respectively), whereas the dehydrocoupling at much higher relative ratios of amine–borane operate at similar rates (see above; 500 equivalents, 0.2 mol % $[\text{Rh}]$, TOF 1150 h^{-1} and 1000 h^{-1} , respectively). This difference in rate may suggest that active-species formation from **1** is dependent on the concentration of amine–borane, possibly aided by outer-sphere B–H \cdots H–N interactions.^[29] Overall, the current data suggest that if not the actual catalyst, dimeric species such as **5** likely sit close to the real catalyst.

In summary, P–C-activated dimeric complexes based upon the $\{\text{Rh}_2(\text{xantphos}')_2\}^{2+}$ motif are very active catalysts for the dehydrocoupling of $\text{H}_3\text{B}\cdot\text{NMe}_2\text{H}$ and the dehydropolymerization of $\text{H}_3\text{B}\cdot\text{NMe}_2\text{H}$. Kinetic data suggest that the mechanisms of dehydrocoupling by dimeric and previously reported monomeric precatalysts may be closely related. The implication that dimeric species are active suggests that bimetallic cooperativity might be important for dehydropolymerization and offers opportunities to further tune catalyst properties as has successfully been demonstrated for olefin polymerization processes.^[8] More generally given the wide use of xantphos as a ligand for many catalytic applications,^[30] it will be interesting to see whether P–C-activated dimers prove to be a common motif in organometallic chemistry.

Keywords: amine–boranes · homogeneous catalysis · P ligands · rhodium · X-ray diffraction

How to cite: *Angew. Chem. Int. Ed.* **2015**, *54*, 10173–10177
Angew. Chem. **2015**, *127*, 10311–10315

- [1] a) E. M. Leitao, T. Jurca, I. Manners, *Nat. Chem.* **2013**, *5*, 817–829; b) H. C. Johnson, T. N. Hooper, A. S. Weller, *Top. Organomet. Chem.* **2015**, *49*, 153–220.
- [2] a) C. W. Hamilton, R. T. Baker, A. Staubitz, I. Manners, *Chem. Soc. Rev.* **2009**, *38*, 279–293; b) A. Staubitz, A. P. M. Robertson, I. Manners, *Chem. Rev.* **2010**, *110*, 4079–4124.
- [3] a) A. Staubitz, A. P. Soto, I. Manners, *Angew. Chem. Int. Ed.* **2008**, *47*, 6212–6215; *Angew. Chem.* **2008**, *120*, 6308–6311; b) A. Staubitz, M. E. Sloan, A. P. M. Robertson, A. Friedrich, S. Schneider, P. J. Gates, J. Gunne, I. Manners, *J. Am. Chem. Soc.* **2010**, *132*, 13332–13345; c) R. Dallanegra, A. P. M. Robertson, A. B. Chaplin, I. Manners, A. S. Weller, *Chem. Commun.* **2011**, *47*, 3763–3765; d) R. T. Baker, J. C. Gordon, C. W. Hamilton, N. J. Henson, P. H. Lin, S. Maguire, M. Murugesu, B. L. Scott, N. C. Smythe, *J. Am. Chem. Soc.* **2012**, *134*, 5598–5609; e) A. N. Marziale, A. Friedrich, I. Klopsch, M. Drees, V. R. Celinski, J. Guenne, S. Schneider, *J. Am. Chem. Soc.* **2013**, *135*, 13342–13355.
- [4] H. C. Johnson, E. M. Leitao, G. R. Whittell, I. Manners, G. C. Lloyd-Jones, A. S. Weller, *J. Am. Chem. Soc.* **2014**, *136*, 9078–9093.
- [5] H. C. Johnson, C. L. McMullin, S. D. Pike, S. A. Macgregor, A. S. Weller, *Angew. Chem. Int. Ed.* **2013**, *52*, 9776–9780; *Angew. Chem.* **2013**, *125*, 9958–9962.
- [6] H. C. Johnson, R. Torry-Harris, L. Ortega, R. Theron, J. S. McIndoe, A. Weller, *Catal. Sci. Technol.* **2014**, *4*, 3486–3494.
- [7] P. W. N. M. v. Leeuwen, J. C. Chadwick, *Homogeneous Catalysis*, Wiley-VCH, Weinheim, **2011**.
- [8] M. Delferro, T. J. Marks, *Chem. Rev.* **2011**, *111*, 2450–2485.
- [9] For the involvement of bimetallic species in the dehydrocoupling of H₃B·NMe₂H see: a) T. Miyazaki, Y. Tanabe, M. Yuki, Y. Miyake, Y. Nishibayashi, *Organometallics* **2011**, *30*, 2394–2404; b) A. B. Chaplin, A. S. Weller, *Angew. Chem. Int. Ed.* **2010**, *49*, 581–584; *Angew. Chem.* **2010**, *122*, 591–594.
- [10] a) H. Werner, B. Klingert, A. L. Rheingold, *Organometallics* **1988**, *7*, 911–917; b) K. Wang, T. J. Emge, A. S. Goldman, *Inorg. Chim. Acta* **1997**, *255*, 395–398.
- [11] H. Nöth, S. Thomas, *Eur. J. Inorg. Chem.* **1999**, 1373–1379.
- [12] A. C. Dunbar, G. S. Girolami, *Inorg. Chem.* **2013**, *52*, 888–896.
- [13] J. C. Green, M. L. H. Green, G. Parkin, *Chem. Commun.* **2012**, *48*, 11481–11503.
- [14] a) R. A. Jones, N. C. Norman, M. H. Seeberger, J. L. Atwood, W. E. Hunter, *Organometallics* **1983**, *2*, 1629–1634; b) R. A. Jones, T. C. Wright, J. L. Atwood, W. E. Hunter, *Organometallics* **1983**, *2*, 470–472.
- [15] a) D. W. Meek, P. E. Kreter, G. G. Christoph, *J. Organomet. Chem.* **1982**, *231*, C53–C58; b) S. Douglas, J. P. Lowe, M. F. Mahon, J. E. Warren, M. K. Whittlesey, *J. Organomet. Chem.* **2005**, *690*, 5027–5035.
- [16] See the Supporting Information.
- [17] G. Alcaraz, S. Sabo-Etienne, *Coord. Chem. Rev.* **2008**, *252*, 2395–2409.
- [18] a) J. Spielmann, S. Harder, *Dalton Trans.* **2011**, *40*, 8314–8319; b) M. Hata, Y. Kawano, M. Shimoi, *Inorg. Chem.* **1998**, *37*, 4482–4483.
- [19] a) N. Merle, G. Koicok-Kohn, M. F. Mahon, C. G. Frost, G. D. Ruggiero, A. S. Weller, M. C. Willis, *Dalton Trans.* **2004**, 3883–3892; b) M. Shimoi, S. Nagai, M. Ichikawa, Y. Kawano, K. Katoh, M. Uruichi, H. Ogino, *J. Am. Chem. Soc.* **1999**, *121*, 11704–11712.
- [20] G. L. Williams, C. M. Parks, C. R. Smith, H. Adams, A. Haynes, A. J. Meijer, G. J. Sunley, S. Gaemers, *Organometallics* **2011**, *30*, 6166–6179.
- [21] R. J. Pawley, G. L. Moxham, R. Dallanegra, A. B. Chaplin, S. K. Brayshaw, A. S. Weller, M. C. Willis, *Organometallics* **2010**, *29*, 1717–1728.
- [22] P. E. Garrou, *Chem. Rev.* **1985**, *85*, 171–185.
- [23] J. A. Dimmer, M. Hornung, T. Wütz, L. Wesemann, *Organometallics* **2012**, *31*, 7044–7051.
- [24] At 0.288 M the loading of **5** is only 0.025 mol %.
- [25] a) P. W. N. M. van Leeuwen, *Appl. Catal. A* **2001**, *212*, 61–81; b) L.-B. Han, T. D. Tilley, *J. Am. Chem. Soc.* **2006**, *128*, 13698–13699.
- [26] P. Buchwalter, J. Rosé, P. Braunstein, *Chem. Rev.* **2015**, *115*, 28–126.
- [27] a) M. D. Fryzuk, W. E. Piers, F. W. B. Einstein, T. Jones, *Can. J. Chem.* **1989**, *67*, 883–896; b) Z. Lu, B. L. Conley, T. J. Williams, *Organometallics* **2012**, *31*, 6705–6714; c) L. J. Sewell, M. A. Huertos, M. E. Dickinson, A. S. Weller, G. C. Lloyd-Jones, *Inorg. Chem.* **2013**, *52*, 4509–4516.
- [28] R. N. Perutz, S. Sabo-Etienne, *Angew. Chem. Int. Ed.* **2007**, *46*, 2578–2592; *Angew. Chem.* **2007**, *119*, 2630–2645.
- [29] A. Kumar, H. C. Johnson, T. N. Hooper, A. S. Weller, A. G. Algarra, S. A. Macgregor, *Chem. Sci.* **2014**, *5*, 2546–2553.
- [30] M.-N. Birkholz, Z. Freixa, P. W. N. M. van Leeuwen, *Chem. Soc. Rev.* **2009**, *38*, 1099–1118.

Received: May 4, 2015

Published online: July 3, 2015